

Dynamics of de novo vitellogenesis in fish with indeterminate fecundity: an application of oocyte packing density theory to European anchovy, *Engraulis encrasicolus*

Eudoxia Schismenou · Stylianos Somarakis ·
Anders Thorsen · Olav S. Kjesbu

Received: 20 April 2011 / Accepted: 3 December 2011 / Published online: 20 December 2011
© Springer-Verlag 2011

Abstract De novo vitellogenesis is common among teleosts; however, its dynamics and the timing of batch recruitment are poorly understood. In this study, we combine a suite of methods and theories in fish reproductive biology (oocyte packing density, stereology, ovarian allometry, oocyte size frequencies and postovulatory follicle [POF] ageing) to reconstruct the steps and timing of batch recruitment in European anchovy. Using general linear modelling to standardize oocyte numbers, we demonstrate that the fractions of primary growth, cortical alveoli and vitellogenic oocytes in the ovary are relatively stable in females with migratory nucleus oocytes (MN) or with POFs 1 and 2 days old (POF-1 and POF-2), but they change abruptly at hydration. These results imply that batch recruitment in European anchovy occurs in pulses of very short duration (less than a day). The standing crop of vitellogenic oocytes in MN, POF-1 and POF-2 females equals the number of eggs contained in two mature batches.

Introduction

Fish are distinguished into determinate and indeterminate spawners according to pattern of oocyte recruitment (Hunter et al. 1992; Murua and Saborido-Rey 2003). In determinate spawners, oocytes to be released in the imminent spawning season are recruited into vitellogenesis once, allowing estimation of annual fecundity at a single point in time prior to spawning. In contrast, indeterminate spawners continuously recruit oocytes into vitellogenesis during the course of the reproductive period (continuous de novo vitellogenesis).

The dynamics of de novo vitellogenesis and batch recruitment in fish with indeterminate fecundity have rarely been examined. In controlled laboratory experiments in which days from spawning were known and using a combination of stereological analysis and measurements of serum sex steroid levels, Coward and Bromage (1998) concluded that previtellogenic oocytes in *Tilapia zillii* are recruited into vitellogenic growth immediately after spawning and can complete vitellogenesis as early as day-8 post-spawning. Recently, Korta et al. (2010) studied batch recruitment in field-caught European hake (*Merluccius merluccius*) by applying the oocyte packing density formula developed by Kurita and Kjesbu (2009). The formula was based on the extension of the auto-diametric method, originally developed for fecundity estimations in determinate spawners (Thorsen and Kjesbu 2001; Witthames et al. 2009). Korta et al. (2010) combined the extended oocyte packing density formula with stereological techniques in an effort to follow the dynamics of oocyte numbers among developmental stages of the oocytes. However, their analysis was restricted to oocyte packing densities (number of oocytes per gram of ovary), that is, changes in ovary weight associated with oocyte development, fish size and

Communicated by C. Harrod.

E. Schismenou (✉) · S. Somarakis
Institute of Marine Biological Resources,
Hellenic Centre for Marine Research,
P.O. Box 2214, 71003 Heraklion, Crete, Greece
e-mail: schismenou@hcmr.gr

E. Schismenou
Department of Biology, University of Crete,
P.O. Box 2208, 71409 Heraklion, Crete, Greece

A. Thorsen · O. S. Kjesbu
Institute of Marine Research, P.O. Box 1870,
5817 Nordnes, Bergen, Norway

fecundity (Jons and Miranda 1997) were not taken into consideration. Nevertheless, to fully document the way that oocyte batches recruit and grow from one stage of development to the next, absolute oocyte numbers have to be estimated after standardizing for relative ovary weight. In the present paper, we extend the analysis of Korta et al. (2010), using European anchovy (*Engraulis encrasicolus*) as the study species, and examine variation in absolute oocyte numbers per stage of oocyte development taking also into account principles of ovarian allometry (Somarakis et al. 2004a).

European anchovy is a small pelagic fish that spawns from spring to autumn, normally from April to September (Somarakis et al. 2004b, 2006). Spawning is highly synchronized and takes place soon after sunset (Somarakis et al. 2004b, 2011). Inter-spawning intervals are typically 2–4 days (Somarakis et al. 2004b, 2011). Females can easily be assigned as to the day of spawning using the postovulatory follicle (POF) method (Ganias et al. 2003; Somarakis et al. 2011; Uriarte et al. 2011).

In the present study, we were particularly interested in addressing the following questions: (a) Does batch recruitment in anchovy occur in pulses and if so how rapid are these pulses? The ability to age POFs in small pelagic fish was likely to highlight the timing of batch recruitment. (b) For how many batches does the number of vitellogenic oocytes in the ovaries of actively spawning fish suffice? In northern anchovy (*Engraulis mordax*), Hunter and Leong (1981) have calculated that the total number of vitellogenic oocytes in the ovaries before spawning is sufficient for two successive batches of eggs. (c) Finally, at which stage of oocyte development can we measure batch fecundity? In northern anchovy, oocyte size frequency distributions are continuous, and the most advanced batch is clearly separated from less developed oocytes at the hydration stage (Hunter and Goldberg 1980; Hunter and Leong 1981; Hunter et al. 1985). However, in other small pelagic fishes like the Mediterranean sardine (*Sardina pilchardus*) (Ganias et al. 2004), a hiatus is established in the oocyte size frequency distributions before oocyte hydration.

Materials and methods

Ovarian sampling and processing

Sampling of female anchovies took place prior to (February, March) and at the beginning (April) of the 2009 spawning season in the North Aegean Sea (Thracian Sea) onboard R/V 'PHILIA' (February) or local purse-seiners (March and April, Table 1). Ovaries were removed immediately after capture and fixed individually in 10% buffered formalin while the remaining parts of the body were frozen

in a plastic bag for subsequent processing in the laboratory. The latter included measurements of thawed eviscerated weight (EW, 0.01 g), total length (TL, mm) and formalin-preserved gonad weight (GW_{formalin} , 0.001 g). An additional sample of 50 females was collected in April 2009 in order to calculate correction factors for formalin-preserved ovary weight using the same protocol as before, but weighing the ovaries both before (GW_{fresh} , 0.001 g) and after fixation.

A subset of 116 fish was selected for histological analyses (Table 1) using random stratified subsampling according to equal categories of $\log(I_G)$, where I_G is relative gonadal index. Consequently, all stages of ovarian maturation were represented (Table 2) but referring only to fish larger than 105 mm (length-at-50% maturity; Somarakis et al. 2006). Histological sections (4 μm) were prepared using historesin as embedding medium and 2% toluidine blue and 1% borax as stain. Ovarian stages were defined based on developmental stage of the most advanced group of oocytes and presence/age of POFs (Hunter and Macewicz 1985) (Table 2). Ageing of POFs (Day-0, Day-1 and Day-2) was based on methods described in Ganias et al. (2003) and Somarakis et al. (2011).

Ovarian density, that is, the ratio between mass and volume ($\rho_o = GW_{\text{formalin}}/GV_{\text{formalin}}$, where GV_{formalin} is ovary volume following preservation), was calculated for 56 of the 116 females having intact ovaries. To estimate ovary volume, the combined ovary displaced weight (m_w) was measured by suspending the fixed ovary in saline water of known density (ρ_w) resting on a balance, that is, using the well-known "Scherle principle" (Emerson et al. 1990), and calculated as $GV_{\text{formalin}} = m_w/\rho_w$. Density of the ovary was then calculated from the weight and volume of each ovary.

Oocyte measurements in whole mounts

Oocyte diameters from each pair of formalin-preserved ovaries were measured from pictures with a resolution of 0.103 pixels/ μm taken with a Micropublisher five RTV Camera (QImaging) mounted on an Olympus SZX 12 microscope using light from underneath from an ILLB200 light stand. The light setting was standardized as detailed in Thorsen and Kjesbu (2001). Oocytes were measured semi-automatically using the open source ImageJ (<http://rsb.info.nih.gov/ij/>) with the plugin ObjectJ (<http://simon.bio.uva.nl/objectj/>). First, large vitellogenic (dark) oocytes were measured using automatic particle analysis, and then, the remaining oocytes (mostly transparent previtellogenic oocytes) with long axes larger than 300 μm were measured manually. Both long (L) and short (S) axes were recorded. Since anchovy oocytes, unlike most other fish species, are ellipsoid, the software that we had previously used for fish with spherical oocytes had to be redesigned. The resulting

Table 1 Date, geographical coordinates, fishing gear and time of sampling of female anchovies

Sample	Date	Latitude, longitude	Fishing gear	Time (h)	N_T	N_H	N_C
1	11/2/2009	40°49'08"N 24°42'75"E	Pelagic trawl	12:45	40	7	–
2	11/2/2009	40°48'80"N 24°43'37"E	Pelagic trawl	14:45	40	1	–
3	17/3/2009	40°50'43"N 25°23'09"E	Purse seine	05:00	100	23	–
4	27/4/2009	40°45'76"N 24°32'28"E	Purse seine	20:30	124	42	50
5	29/4/2009	40°46'92"N 24°32'83"E	Purse seine	02:30	150	43	–

N_T Total number of fish sampled, N_H number of fish used in histological analysis, N_C number of fish used for the calculation of a fresh weight correction factor for formalin-preserved ovary weight

Table 2 Ovarian stages defined based on maturity stage of the most advanced oocytes and presence/age of postovulatory follicles (POFs)

Ovarian phase	Ovarian stage (GONAD)	Oocyte stage (OOCYTE)	WM	OPD (OPD_N)
Immature	Primary growth, PG	PG, ellipsoid primary growth oocytes with homogenous cytoplasm	–	10
Developing (Early developing subphase)	Yolk vesicle, CA	CA, previtellogenic oocytes with yolk vesicles or cortical alveoli formed	–	8 (2)
Developing	Early vitellogenic, EVTO	EVTO, early vitellogenic oocytes with yolk granules in the periphery of cytoplasm	–	7 (1)
Spawning capable	Vitellogenic, VTO	VTO, vitellogenic oocytes with yolk granules all over the cytoplasm	20	11 (4)
Spawning capable (Actively spawning subphase)	Late vitellogenic, MN	MN, vitellogenic oocytes with migrating nucleus	27	10 (10)
Spawning capable (Actively spawning subphase)	Hydrated, HYD	HYD, hydrated oocytes	6	5 (4)
Spawning capable	Day-0 POFs, POF0 (spawned the night of sampling)	VTO, vitellogenic oocytes with yolk granules all over the cytoplasm	2	2
Spawning capable	Day-1 POFs, POF1 (spawned the previous night)	VTO, vitellogenic oocytes with yolk granules all over the cytoplasm	12	12 (2)
Spawning capable	Day-2 POFs, POF2 (spawned two nights before sampling)	MN, vitellogenic oocytes with migrating nucleus	7	7 (1)

WM numbers of ovaries used in whole-mount oocyte measurements for the estimation of oocyte size frequency distributions; OPD (OPD_N) number of ovaries used for theoretical (and gravimetric, in parentheses) oocyte packing density estimations. Corresponding ovarian phases, as described by Brown-Peterson et al. (2011), are also indicated

software is described in more detail and can be downloaded from (<http://simon.bio.uva.nl/objectj/examples/oocytes/Oocytes.htm>).

Oocyte packing density

Oocyte packing density (OPD) was estimated theoretically (Kurita and Kjesbu 2009) (see next paragraph) for each oocyte stage occurring in the gonad in a representative set of 72 gonads (Table 2). Furthermore, the gravimetric oocyte packing density (OPD_N) was calculated according to Thorsen and Kjesbu (2001) for a subset of 24 females for comparison with OPD: from each ovary, two subsamples

were dissected out, weighed (0.01 mg) and all oocytes with long diameter larger than 300 μm were measured (long and short diameter; see previous section) and counted.

For OPD (theoretical packing density), we used the equation of Korta et al. (2010), that is, estimations were performed separately for each oocyte stage i :

$$\log(OPD_i) = \log \left[V_{Vi} \times \left(\frac{1}{\rho_o} \right) \times \left\{ \frac{(1+k)^3}{8 \times k} \right\} \right] + 12.28 - 3 \times \log(OD_{Vi})$$

where OPD_i = number of stage i oocytes per gram of ovary, g^{-1} ; V_{Vi} = volume fraction of stage i oocytes;

ρ_o = ovarian density, g cm^{-3} ; k = mean ratio of long (L) to short (S) diameter of stage i oocytes; OD_{Vi} = volume-based mean oocyte diameter of stage i oocytes, μm . The sum of OPD_i of all oocyte stages in the ovary was the total number of oocytes per gram of ovary (OPD).

Stereological analysis

Volume fraction and volume-based oocyte diameter

The volume fraction of stage i oocytes (V_{Vi}) in the ovary was estimated according to the Delesse principle, that is, considering that area fractions are proportional to volume fractions (Howard and Reed 1998). For stereological analysis, a standard grid of 256 points and five counting fields per individual were used (Korta et al. 2010). Total count of grid points per field ranged from 58 (in sections of PG ovaries) to 256 (in sections of HYD and POF2 ovaries) (see Table 2 for abbreviations). In each gonad, V_{Vi} was estimated for every oocyte stage present in the ovary, from PG to HYD, and for ‘other’ which included ovarian wall, stroma and post-ovulatory follicles. Additionally, V_{Vi} was estimated for the smaller, spherical primary growth oocytes with densely stained cytoplasm (PG-S). V_V was calculated as the sum of V_{Vi} from PG to the most advanced oocyte stage (i.e. excluding PG-S).

In the same histological preparations, the long (L) and short (S) diameters were measured manually for the 2–15 largest oocytes of each stage i , from PG to HYD, in each female. These measurements were used for the estimation of individual oocyte diameter ($\text{OD}_{(\text{ind})} = (L + S)/2$), L/S ratio, ‘volume-based mean’ oocyte diameter (OD_{Vi}) and ‘arithmetic mean’ oocyte diameter (OD_{Ni}) in stage i (Kurita and Kjesbu 2009; Korta et al. 2010):

$$\text{OD}_{Vi} = \left[\sum_{j=i}^{n_i} \left(\frac{(\text{OD}_{(\text{ind})i,j})^3}{n_i} \right) \right]^{\frac{1}{3}}, \quad \text{OD}_{Ni} = \sum_{j=i}^{n_i} \frac{\text{OD}_{(\text{ind})i,j}}{n_i}$$

Subsequently, the volume-based mean oocyte diameter (OD_V) and the number-based mean oocyte diameter (OD_N), weighted by oocyte packing densities, were estimated for each female:

$$\text{OD}_V = \left[\sum_i \left(\frac{\text{OD}_{Vi}^3 \times \text{OPD}_i}{\text{OPD}} \right) \right]^{\frac{1}{3}}, \quad \text{OD}_N = \sum_i \frac{\text{OD}_{Ni} \times \text{OPD}_i}{\text{OPD}}$$

Correction for oocyte shrinkage

The diameter measurements (L, S) performed on slides were corrected for shrinkage during histological processing in order to represent the actual dimensions in formalin-preserved ovaries.

From oocyte measurements performed in whole mounts, the 10 largest oocytes per ovary were averaged (L and S for long and short diameter, respectively). These averages were then regressed against the mean dimensions of the most advanced stage of oocytes from measurements in histological sections (L_H and S_H) of the same ovaries. Resultant equations, including oocyte stage as a fixed factor (i.e. analysis of covariance models), were then used to convert histological diameters to formalin-preserved diameters.

Calculation of oocyte numbers in the whole ovary

Number of stage i oocytes (N_i) in each individual was calculated from OPD_i and gonad weight as: $N_i = \text{OPD}_i \times \text{GW}_{\text{formalin}}$. However, ovary weight, apart from ovarian stage (mean oocyte size), depends also on fish size (ovarian allometry) and fish fecundity (Jons and Miranda 1997; Somarakis et al. 2004a). For proper comparisons, the N_i should therefore be adjusted for the effect of relative ovary weight using an appropriate gonadal index (Erickson et al. 1985; Somarakis et al. 2004a). Specifically, the allometric relationship between ovary weight (GW_{fresh}) and eviscerated weight (EW) was modelled first and tested for homogeneity of slopes between the different ovarian stages (GONAD):

$$\log(\text{GW}_{\text{fresh}}) = a + b_1 \times \log(\text{EW}) + b_2 \times (\text{GONAD}) + b_3 \times (\text{GONAD}) \times \log(\text{EW})$$

Common slope (b) was then used to calculate the relative gonadal index, that is, $I_G = \text{GW}_{\text{fresh}}/\text{EW}^b$ (Erickson et al. 1985), which accounts for ovarian allometry (Somarakis et al. 2004a).

In the subsequent step of the analysis, adjusted means of stage i oocyte numbers (N_i) and their 95% confidence intervals were estimated for each ovarian stage (GONAD)—oocyte stage (OOCYTE) combination using a general linear model (GLM):

$$\log(N_i) = a + b_1 \times (\text{GONAD}) \times (\text{OOCYTE}) + b_2 \times \log(I_G) + b_3 \times (\text{OOCYTE}) \times \log(I_G)$$

The selection of interaction terms to include in the model was based on prior exploratory analysis (not shown here). The latter showed that the slope of the N_i -on- I_G relationship changed significantly between oocyte stages ($F_{(1,5)} = 3.24$, $P = 0.008$), implying the inclusion of an interaction term, namely $(\text{OOCYTE}) \times \log(I_G)$, in the final model. The GLM analysis was performed only for ovaries containing fully yolked oocytes (VTO and beyond), after examination of the OPD results.

Finally, the model was validated using information from oocyte size frequency distributions estimated from actual measurements in the whole mounts (Table 2). Specifically, the ratio of the number of oocytes with $OD_{(ind)} > 400 \mu\text{m}$ (VIT_{400}) to the total number of oocytes measured (all oocytes with long axis $> 300 \mu\text{m}$, $Total_{WM}$) was calculated for each fish. Hydrated oocytes were not included in VIT_{400} . The threshold value of $400 \mu\text{m}$ included most vitellogenic oocytes of anchovy (see “Results” section). The ratio $VIT_{400}/Total_{WM}$ was averaged for the VTO, POF0, POF1, POF2, MN and HYD ovarian stages and then regressed against the GLM-predicted ratio of vitellogenic to the total number of oocytes. The rationale was that if the model produced accurate predictions of the number of vitellogenic oocytes, the two independently derived ratios should be highly correlated.

Results

Correction factors and ovarian density

Ovary weight increased significantly due to fixation and preservation in formalin. The relationship between fresh gonad weight (GW_{fresh}) and formalin-preserved gonad weight ($GW_{formalin}$) was best explained by a power (log–log) function (compared to alternative models) in terms of explanation of variation (higher coefficient of determination) and properties of the residuals (randomly distributed, homoscedacity):

$$GW_{fresh} = 0.8095 \times GW_{formalin}^{1.079} (r^2 = 0.99, F_{1,48} = 4641.38, P < 0.001).$$

Histological processing induced oocyte shrinkage (Fig. 1). Analyses of covariance (ANCOVAs) indicated that the slopes of the L-on- L_H and S-on- S_H regressions were homogeneous (L: ANCOVA, $F_{(1,5)} = 1.57, P = 0.187$; S: ANCOVA, $F_{(1,5)} = 0.34, P = 0.888$), but intercepts differed significantly between oocyte stages (L: ANCOVA, $F_{(1,5)} = 4.6, P = 0.001$; S: ANCOVA, $F_{(1,5)} = 10.33, P < 0.001$). Hence, we used the respective ANCOVA models to correct for shrinkage (Fig. 1):

$$L = 146.008 + 0.851 \times L_H + 1 \times (\text{Stage} = \text{PG}) + 25.922 \times (\text{Stage} = \text{CA}) + 109.598 \times (\text{Stage} = \text{EVTO}) + 99.668 \times (\text{Stage} = \text{VTO}) + 72.010 \times (\text{Stage} = \text{MN}) + 163.778 \times (\text{Stage} = \text{HYD}), (\text{adjusted } r^2 = 0.974, N = 62)$$

$$S = 50.716 + 0.871 \times S_H + 1 \times (\text{Stage} = \text{PG}) + 14.999 \times (\text{Stage} = \text{CA}) + 78.781 \times (\text{Stage} = \text{EVTO}) + 75.711 \times (\text{Stage} = \text{VTO}) + 71.744 \times (\text{Stage} = \text{MN}) + 150.597 \times (\text{Stage} = \text{HYD}), (\text{adjusted } r^2 = 0.980, N = 62)$$

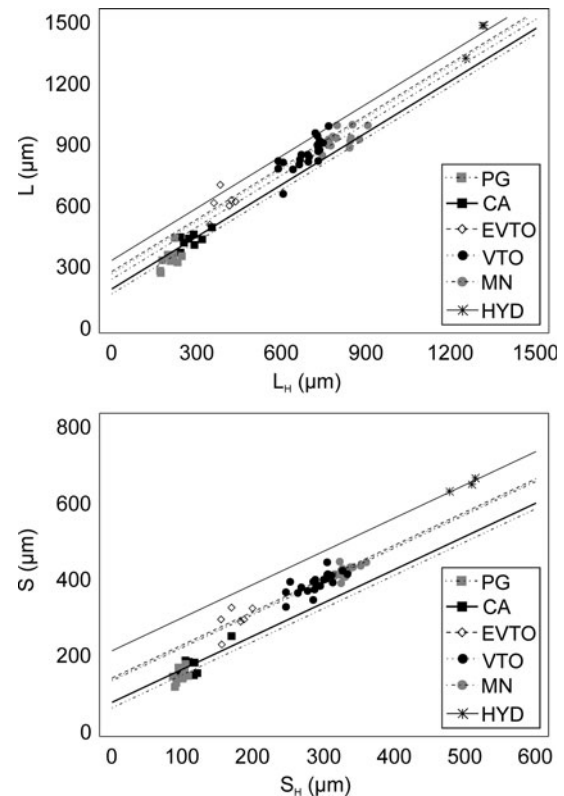


Fig. 1 Plots of the analysis of covariance models for the correction of long (L_H) and short oocyte diameter (S_H) for shrinkage due to histological processing. L and S: formalin-preserved long and short diameters, respectively. Abbreviations of oocyte stages are defined in Table 2

The shrinkage-corrected diameters were subsequently used for the calculation of all parameters related with OPD ($OD_{(ind)}, L/S, OD_{Vi}, OD_{Ni}, OD_V, OD_N$).

Ovarian density was quite variable, but analysis of variance indicated that there were no significant differences in mean density between ovarian stages (ANOVA, $F_{(8,47)} = 0.34, P = 0.945$). To conform to previous studies on oocyte packing density (Kurita and Kjesbu 2009; Korta et al. 2010), we used different mean values of ovarian density for non-vitellogenic (PG and CA; 1.051 g cm^{-3} , $N = 20$), vitellogenic (EVTO, VTO, MN, POF0, POF1 and POF2; 1.109 g cm^{-3} , $N = 34$) and hydrated gonads (HYD; 1.072 g cm^{-3} , $N = 2$).

Oocyte size

Vitellogenic oocytes were generally larger than $400 \mu\text{m}$ in diameter. Specifically, the volume-based oocyte diameter (OD_{Vi}) averaged $X \pm SD = 236 \pm 12 \mu\text{m}$, $N = 72$, in PG and $315 \pm 18 \mu\text{m}$, $N = 62$, in CA. For vitellogenic stages, OD_{Vi} averaged $454 \pm 21 \mu\text{m}$, $N = 54$; $576 \pm 51 \mu\text{m}$, $N = 44$ and $664 \pm 26 \mu\text{m}$, $N = 17$, for EVTO, VTO and

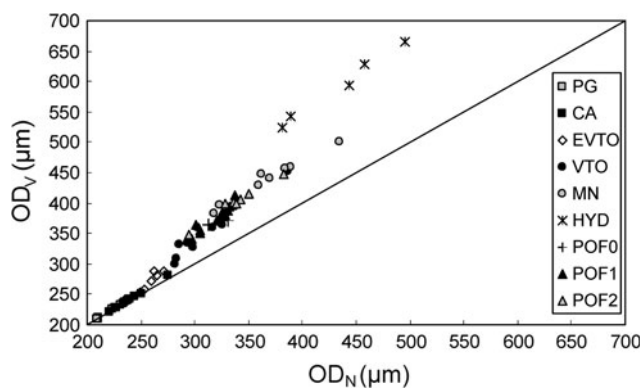


Fig. 2 Relationship between number-based mean oocyte diameter (OD_N) and volume-based mean oocyte diameter (OD_V) at different ovarian stages. The line indicates a 1:1 relationship. Abbreviations of ovarian stages are defined in Table 2

MN, respectively. In hydrated oocytes (HYD), mean OD_{V_i} was $1,026 \pm 21 \mu\text{m}$, $N = 5$.

Plotting the volume-based mean oocyte diameter (OD_V) against the number-based mean oocyte diameter (OD_N) revealed an increasing divergence with advancing ovarian growth (Fig. 2). The difference was very small for non-vitellogenic ovarian stages (maximum 7 μm in PG and CA), but in vitellogenic stages (presence of yolked oocytes and/or POFs), OD_V was much higher than OD_N (up to 86 μm). In hydrated ovaries, the difference almost doubled (142–171 μm).

Volume fraction

The volume fraction of oocytes in the ovary (V_V) increased with increasing OD_V (Fig. 3). The increase was most sharp

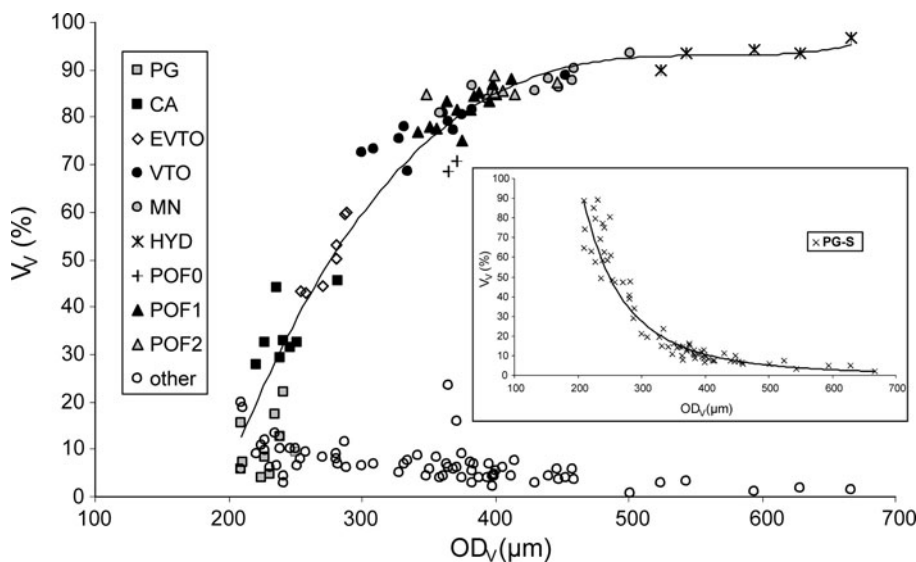


Fig. 3 Oocyte volume fraction (V_V) of different ovarian stages (fitted line: 3rd-order polynomial regression). Other: volume fraction of ovarian wall, stroma and postovulatory follicles. Inset figure: volume

(from 0.04 to 0.59) in a narrow range of OD_V (210–287 μm) corresponding to oocyte growth from the PG to EVTO stage. Subsequent yolk accumulation (OD_V 300–667 μm) was associated with a lower rate of V_V increase, up to an asymptotic level in hydrated ovaries (maximum V_V 0.97). Females that had spawned the night of the sampling (POF0) had lower V_V than females in POF1 or VTO. Furthermore, in POF0 ovaries, the fraction of ‘other’ was higher due to the presence of new postovulatory follicles. The evolution of volume fraction of PG-S (small, spherical primary growth oocytes) exhibited a trend opposite to that of V_V .

Oocyte packing density

The gravimetric (OPD_N) and the theoretically estimated (OPD) oocyte packing density exhibited the same general pattern with regard to mean oocyte size, but the latter resulted in much higher figures (Fig. 4). At advanced ovarian stages (from VTO to HYD), packing density decreased steadily with increasing oocyte size. At earlier ovarian stages, oocyte packing density was generally increasing with advancement of maturation.

When considering ovarian stages beyond the EVTO, the log(OPD_N)-on-log(OD_N), and especially the log(OPD)-on-log(OD_V), linear regressions had very good fits (not shown; r^2 values: 0.869 and 0.984, respectively). For the latter relationship, analysis of covariance indicated homogeneous slopes between ovarian stages (ANCOVA, $F_{(1,6)} = 0.99$, $P = 0.438$), but the intercept of the POF0 stage was significantly lower ($t_{44} = 4.398$, $P < 0.001$). The final

fraction of small spherical primary growth oocytes (PG-S) not considered in V_V (fitted line: power regression)

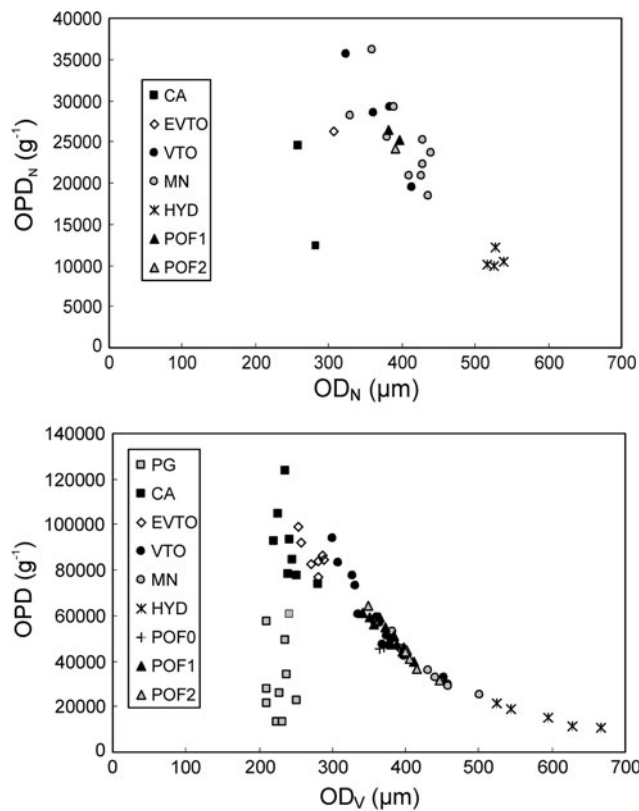


Fig. 4 Upper panel Gravimetric oocyte packing density (OPD_N) against number-based oocyte diameter (OD_N). Lower panel Theoretical oocyte packing density (OPD) against volume-based mean oocyte diameter (OD_V). Abbreviations of ovarian stages are defined in Table 2

relationship (Fig. 5) was very strong (ANCOVA, $F_{(1,1)} = 1,946.28$, $P < 0.001$, adjusted $r^2 = 0.988$).

Number of stage i oocytes

Ovary weight (GW_{fresh}) was significantly related to eviscerated weight (EW) in all ovarian stages. The slopes for all models were homogeneous (ANCOVA, $F_{(1,8)} = 1.58$, $P = 0.154$), but intercepts were significantly different (ANCOVA, $F_{(1,8)} = 38.78$, $P < 0.001$). Subsequently, the

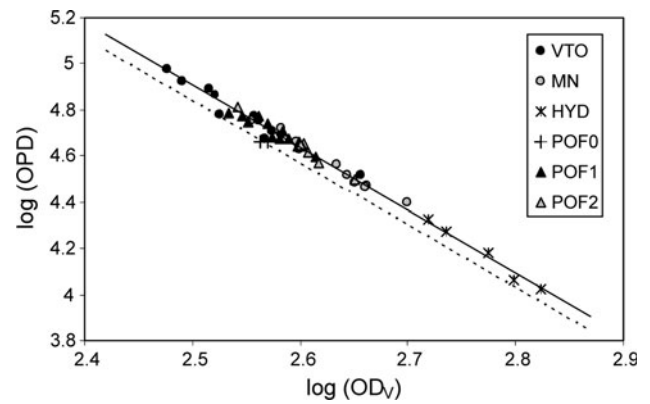


Fig. 5 Plot of the analysis of covariance model between theoretical oocyte packing density (OPD) and volume-based mean oocyte diameter (OD_V) for females in ovarian stage VTO and beyond. The dashed line corresponds to POF0 females

common slope of the ANCOVA model ($b = 1.76$) was used for the calculation of the relative gonadal index.

The GLM analysis of the number of stage i oocytes (N_i) included ovaries from stage VTO and beyond, that is, ovaries that had been fully recruited to the current reproductive period. The model was highly significant and explained 84% of variation in the number of stage i oocytes (Table 3). Estimates of N_i and their coefficients of variation (CVs) are presented in Table 4.

The numbers of yolk vesicle and yolked oocytes (VIT) were lower in VTO ovaries (Table 4) compared to the other vitellogenic ovarian stages with signs of past or imminent spawning (POF0, POF1, POF2 and MN). Probably, the recruitment of vitellogenic oocytes was not yet completed, at least in a subset of the VTO females, implying that they had not yet reached full maturity, that is, they were not active spawners.

Predictions of oocyte numbers for hydrated gonads were less precise (Table 4, CVs), especially for the number of hydrated oocytes (HYD). However, the predicted number of hydrated oocytes was similar to the number of migratory nucleus oocytes (MN) in POF2 and MN ovaries ($\sim 4,000$ oocytes, Table 4). An inspection of oocyte size frequency

Table 3 ANOVA table for GLM for number of oocytes in stage i , $\log(N_i)$, showing predictors and associated statistical indices

Source	Type III SS	df	Mean SS	F	P
Corrected model	25.940	32	0.811	33.927	<0.001
Intercept	495.228	1	495.228	20,727.130	<0.001
GONAD \times OOCYTE	6.057	26	0.233	9.750	<0.001
$\log(I_G)$	0.163	1	0.163	6.804	0.010
OOCYTE \times $\log(I_G)$	0.590	5	0.118	4.939	<0.001
Error	4.157	174	0.024		
Total	2,781.748	207			
Corrected total	30.097	206			
	Adjusted $r^2 = 0.836$				

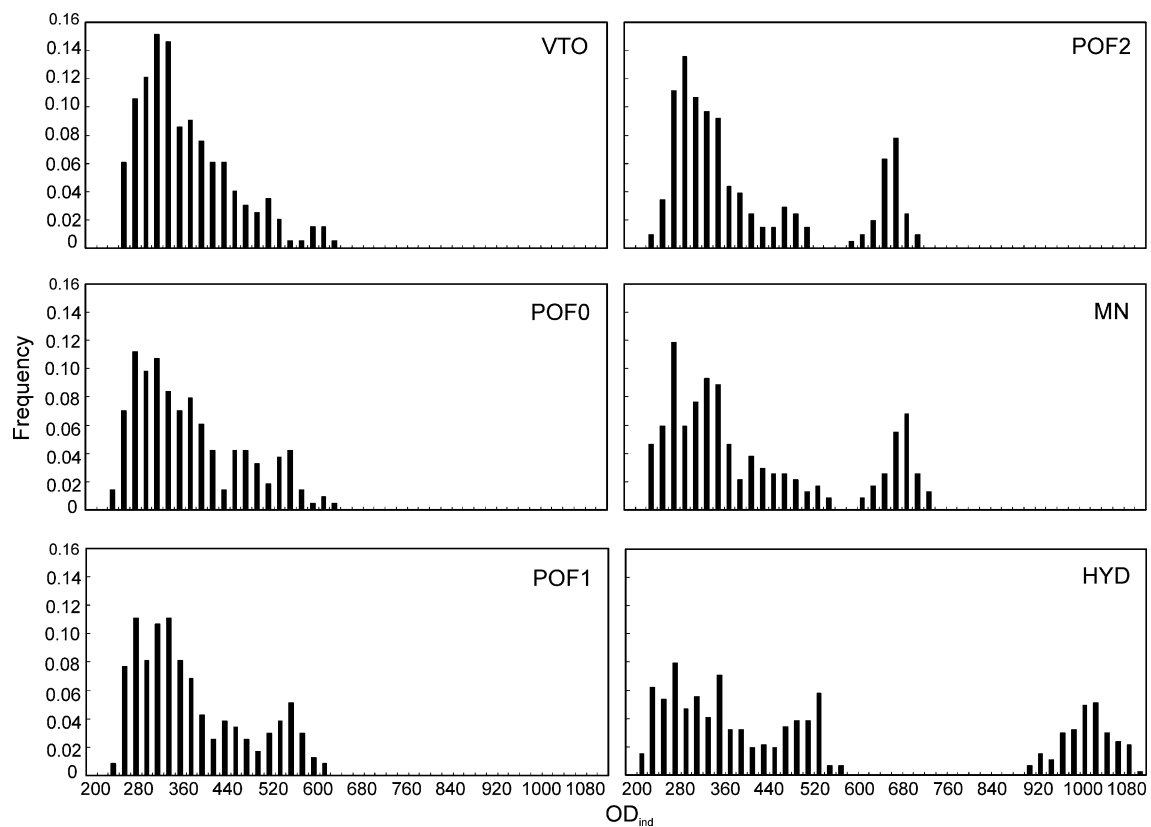


Fig. 6 Examples of oocyte size (OD_{ind}) frequency distributions for individuals in different ovarian stages

Table 4 GLM estimates of $\log(N_i)$ for each ovarian stage along with their coefficients of variation, CVs (in parentheses)

Oocyte stage	Ovarian stage					
	VTO	POF0	POF1	POF2	LVTO	HYD
$\log(N_i)$						
PG	4.190 (0.013)	4.215 (0.026)	4.205 (0.011)	4.215 (0.014)	4.184 (0.012)	4.070 (0.023)
CA	3.539 (0.016)	3.705 (0.030)	3.646 (0.012)	3.644 (0.016)	3.622 (0.014)	3.707 (0.025)
EVTO	3.395 (0.017)	3.561 (0.031)	3.586 (0.013)	3.479 (0.017)	3.444 (0.014)	3.239 (0.028)
VTO	3.414 (0.017)	3.547 (0.031)	3.601 (0.013)	2.943 (0.020)	3.181 (0.017)	3.139 (0.032)
LVTO				3.583 (0.016)	3.623 (0.014)	
HYD						3.630 (0.072)
N_i						
PG	15,486	16,407	16,016	16,409	15,288	11,742
CA	3,457	5,074	4,431	4,405	4,192	5,096
EVTO	2,481	3,643	3,859	3,013	2,778	1,733
VTO	2,594	3,525	3,991	876	1,518	1,378
LVTO				3,830	4,196	
HYD						4,266
VIT	5,075	7,167	7,850	7,720	8,492	3,111
Total	24,018	28,649	28,296	28,534	27,972	24,215

The back-transformed (antilog) values of the estimates (N_i) are also presented

VIT number of oocytes in vitellogenesis (VIT = EVTO + VTO + MN), Total sum of oocytes from PG to HYD

distributions (based on diameter measurements in whole mounts) of individual females at different stages of ovarian development revealed that, when oocyte maturation begins

(in females with migratory nucleus oocytes in the ovary, namely POF2 and MN), a clear hiatus develops between the spawning batch and the stock of less developed oocytes

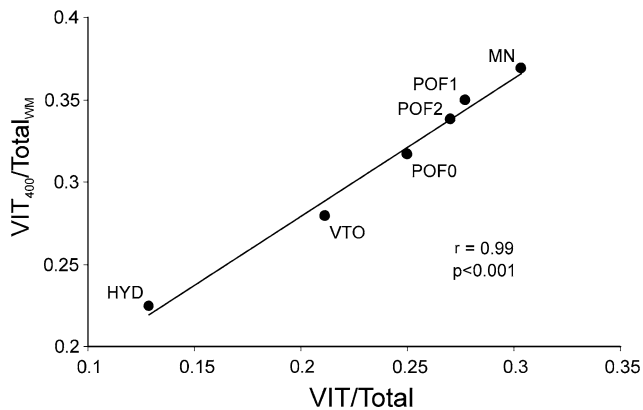


Fig. 7 Validation of the GLM model from theoretical oocyte packing density application using oocyte measurements in whole mounts. Comparison of the ratio $VIT/Total$, calculated from Table 4, against the ratio $VIT_{400}/Total_{WM}$. VIT_{400} : number of oocytes with $OD_{ind} > 400 \mu m$ in whole-mount measurements. $Total_{WM}$: Total number of oocytes (i.e. oocytes with long diameter $> 300 \mu m$) in whole-mount measurements

(Fig. 6). Similar predictions of batch size in POF2, MN and HYD ovaries implied high accuracy of the GLM model. This was further validated by the high correlation (Pearson correlation coefficient: $r = 0.99$) between the ratio $VIT/Total$ (calculated from the GLM estimates presented in Table 4) and the independently derived $VIT_{400}/Total_{WM}$ (Fig. 7).

When the spawning batch enters into oocyte maturation (POF2, MN ovaries), the number of VTO oocytes in the ovaries decreases (Table 4). However, total number of vitellogenic oocytes ($VIT = EVTO + VTO + MN$) in the ovaries of POF2, MN, but also POF1, was similar ($\sim 8,000$) and almost equalled two times the number of oocytes in the batch (batch fecundity). Indeed, the ratio of migratory nucleus oocytes to total vitellogenic oocytes was almost 0.5 in both MN and POF2.

A clearer picture of the timing of batch recruitment was obtained when the ratios of $PG/Total$, $CA/Total$ and $VIT/Total$ were examined for actively spawning fish (Fig. 8). In fish that have spawned 1 and 2 days before (POF1 and POF2), these ratios were similar. This was also true for the sample of MN females with the exception of a higher ratio for VIT vs lower ratio for PG oocytes. In hydrated ovaries, the ratio of vitellogenic oocytes decreased (due to hydration of the spawning batch), but concurrently, the PG oocytes also decreased while CAs increased. The changes observed in hydration were rapidly compensated, and POF0 females had ratios closer to POF1 and POF2 females.

Discussion

In this paper, we applied advanced methods and theories of fish reproductive biology (oocyte packing density,

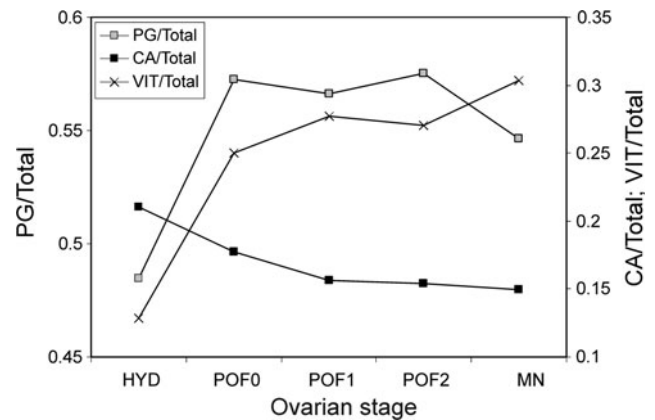


Fig. 8 Ratios of PG, CA and VIT on total number of oocytes calculated from Table 4 only for actively spawning fish

stereology, ovarian allometry, oocyte size frequencies and postovulatory follicle ageing) (Kurita and Kjesbu 2009; Witthames et al. 2009; Somarakis et al. 2004a) and general linear modelling in order to study the dynamics of vitellogenesis in an indeterminate spawner from samples collected in the field. The combination of these methods allowed for a detailed representation of the course of batch generation in anchovy.

In this study, the smallest oocytes used for the estimation of the theoretical OPD were the PG with long diameter $> 300 \mu m$. Kurita and Kjesbu (2009) measured early vitellogenic oocytes larger than $290 \mu m$ for the Japanese flounder (*Paralichthys olivaceus*), whereas Korta et al. (2010) extended their analysis down to small previtellogenic oocytes with diameter $> 90 \mu m$ in the European hake. Thus, in anchovy and the Japanese flounder, OD_N and OD_V exhibited increasing divergence with the advancement of ovarian maturation (e.g. Fig. 2), but in European hake, differences were negligible due to the predominance of the smaller oocytes in the ovaries across all maturity stages (Korta et al. 2010).

Similarly, the gravimetric and theoretical OPD in anchovy had comparable patterns (increasing up to the VTO stage and subsequently decreasing, Fig. 4) to those of the theoretical OPD of the Japanese flounder and the gravimetric OPD of the European hake. However, in hake, the theoretical OPD constantly decreased with OD_V , and oocyte estimates at early stages were much higher as a result of the inclusion of very small previtellogenic oocytes.

Since in this study and the study of Kurita and Kjesbu (2009), only oocytes larger than 300 and $290 \mu m$ were used to estimate OPD, we interpret this pattern of increasing OPD with increasing OD up to the VTO stage as the initial phase of recruitment of oocytes into the current reproductive period from the pool of smaller primary growth

oocytes that exist in the ovary during the immature or regenerating period. This is further supported by the opposite trends of the volume fraction of the PG-S and that of the developing oocytes (Fig. 3), which respectively decreased and increased steeply up to the VTO stage.

Beyond the VTO stage, OPD decreased steadily and a strong power function was established between OPD and OD (Fig. 5, log-transformed data). In fish with determinate annual fecundity, a similarly strong power function links the number of vitellogenic oocytes per gram ovary with OD (Thorsen and Kjesbu 2001; Kurita and Kjesbu 2009; Witthames et al. 2009) because oocytes to be spawned have already been recruited, that is, their number has been determined. Accordingly, in anchovy, when ovaries reach some point in the VTO stage and are spawning capable (i.e. they are fully recruited to the current spawning period), they contain a number of developing oocytes that keep constant, expect for short periods (pulses) when new batches recruit.

In POF0 ovaries (few hours after spawning), both OPD (Fig. 5) and V_V (Fig. 3) were lower, while the volume fraction of ‘other’ was increased compared to other stages (Fig. 3). In other words, oocyte packing density was reduced immediately after egg release, and the resultant empty space was temporarily occupied by the newly formed (large) postovulatory follicles.

The $\log(\text{OPD})\text{-}\log(\text{OD}_V)$ relationship (Fig. 5) was very strong ($r^2 = 0.99$), in contrast to the studies in other indeterminate spawners (Japanese flounder: Kurita and Kjesbu 2009; European hake: Korta et al. 2010) in which the relationships had higher variation about the fitted regression lines. This is attributable to the narrow sampling window of this study (prior to and at the beginning of the spawning season, rather than at different times along the spawning period) that probably minimized variation in OPD due to seasonal changes in egg size and batch fecundity (Hunter and Leong 1981; Alheit 1989; Clarke 1989; Luo and Musick 1991; Motos 1996; Funamoto and Aoki 2002; Castro et al. 2009).

According to postovulatory follicle size and degree of degeneration and given that samples were collected only during nighttime in April (Table 1), females with POFs were assigned to three daily spawning classes with methods described in previous papers (Ganias et al. 2003; Somarakis et al. 2011). Considering that spawning takes place in early night and peaks at around 2.5 h after sunset (Kawaguchi et al. 1990), that is, at approximately 22:00 h in April, we conclude that full POF resorption was taking more than 52 h, that is, its duration was longer than the <43 h calculated from the Daily Egg Production Method surveys in June (Somarakis et al. 2011) with high surface temperatures (>20°C). The inferred POF duration

in April is in general agreement with that of 55–60 h at 13–19°C calculated from laboratory experiments in the Bay of Biscay (Alday et al. 2008).

Standardizing for relative ovary size, the general linear model produced estimates that indicated a dynamic equilibrium in relative numbers of oocytes across the different stages, at least in the actively spawning stages, defined here as these with signs of imminent or past spawning, that is, excluding VTO ovaries (Table 4). The high correlation ($r = 0.99$) between estimates of the relative number of vitellogenic oocytes derived from the GLM and oocyte measurements in whole mounts (Fig. 7) implied a high accuracy of the methods employed despite the rather small number of fish analysed stereologically.

The GLM estimates of oocyte numbers in HYD ovaries were less precise than in other ovarian stages (Table 4). Shrinkage of hydrated oocytes is significantly higher during the dehydration phase of histological processing (Fig. 1), and many of them do not remain intact; hence, stereological methods might be less precise for hydrated ovaries. However, mean batch size estimates were similar in MN, POF2 and HYD ovaries (~4,000 eggs, Table 4) and comparable to previous batch fecundity estimates in the North Aegean Sea (Somarakis 2005; Somarakis et al. 2011) which implied that, albeit imprecise, the GLM estimate of the number of hydrated oocytes was quite accurate.

The oocyte size frequency distributions for individual females revealed that the differentiation of the batch to be spawned in the next spawning event was evident as soon as 24 h after spawning (POF1 ovaries), and in POF2 and MN ovaries (both containing migratory nucleus oocytes that would be spawned the subsequent night), a clear hiatus was established between the advanced (spawning) batch and the smaller, developing oocytes (Fig. 6). In northern anchovy, Bay anchovy (*Anchoa mitchilli*) and Japanese (*Engraulis japonicus*) anchovy, a size hiatus in the oocyte size frequency distributions is only established at the hydration stage (Hunter and Leong 1981; Luo and Musick 1991; Imai and Tanaka 1994), while in the Mediterranean sardine, at the tertiary yolk globule stage (Ganias et al. 2004). It is likely that oocyte measurements in whole mounts and the use of $\text{OD}_{\text{ind}} ((L + S)/2)$ instead of major oocyte diameter provide more accurate and realistic representations of oocyte sizes that permitted the visualization of the size hiatus before the hydration stage. The advancement of the software used in oocyte measurements in whole mounts for species with elliptic eggs may therefore provide an alternative for measuring batch fecundity in anchovy at stages earlier than hydration [which lasts few hours in European and other summer spawning anchovies (e.g. Motos 1996)] in the case of scant hydrated ovaries in the samples (e.g. Palomera and Pertierra 1993).

In northern anchovy, Hunter and Leong (1981) calculated that the number of vitellogenic oocytes in ovaries with no signs of recent spawning (no POFs) was about two times the actual spawning batch. This is in line with our finding for European anchovy that in POF1, POF2 and MN ovaries, the total number of vitellogenic oocytes equalled two times the spawning batch (Table 4).

The timing of batch recruitment in *E. encrasicolus* was better understood when the ratios of PG/Total, CA/Total and VIT/Total were examined in HYD (just before spawning), POF0 (immediately to few hours after spawning), POF1 (about 24 h post-spawning), POF2 (48 h post-spawning but also 24 before spawning) or MN (about 24 h before spawning) (Fig. 8). Here, it must be acknowledged that the presence of POFs and the assignment of females as to the night of spawning greatly assisted in highlighting the timing of batch recruitment. Furthermore, nucleus migration that begins about 1 day before ovulation in anchovy (Hunter and Macewicz 1985; Motos 1996) permitted the assessment of ovarian dynamics for fish that would spawn in about 24 h.

The observed changes in relative oocyte numbers illustrated in Fig. 8 indicate that batch recruitment in European anchovy is not continuous but rather occurs in rapid pulses of less than 24-h (possibly few hours) activated by the hydration of the spawning batch. The number of oocytes in the ovaries is thereafter in a steady (equilibrium) state, containing two potential spawning batches, until the next event of hydration triggers the subsequent recruitment pulse.

Summarizing, the present combination of state of the art methods and theories in fish reproductive biology allowed for a detailed, original representation of the fast batch recruitment and dynamics of de novo vitellogenesis in an indeterminate spawner with short inter-spawning intervals. We believe that the approach adopted here will be particularly useful in future investigations on the effects of factors such as fish size/age, somatic condition, spawning history, temperature regime and food availability on reproductive potential of indeterminate spawners.

Acknowledgments This work was a Short Term Scientific Mission (STSM) within the EU COST Action ‘FRESH’: Fish Reproduction and Fisheries (FA0601). The STSM was hosted by the IMR, Bergen. The authors would like to thank Bente Njøs Strand at IMR for technical advice. We are particularly grateful to Dr. Argyris Kallianiotis and the staff of the Fisheries Research Institute (FRI-NAG-REF) in Kavala, Greece for their help and for providing laboratory facilities and other resources during the first author’s stay in Kavala to sample onboard the commercial purse seine fleet. The work was also partly funded by the EU Project SARDONE (Improving assessment and management of small pelagic species in the Mediterranean, FP6-44294). Thanks are due to the HCMR responsible scientist for SARDONE, Dr. A. Machias. Finally, the authors would like to thank the two anonymous referees for their constructive comments.

References

- Alday A, Uriarte A, Santos M, Martín I, de Murguía AM, Motos L (2008) Degeneration of postovulatory follicles of the Bay of Biscay anchovy (*Engraulis encrasicolus* L.). *Sci Mar* 72:565–575. doi:10.3989/scimar.2008.72n3565
- Alheit J (1989) Comparative spawning biology of anchovies, sardines, and sprats. *Rapp P.-v. Réun Cons int Explor Mer* 191:7–14
- Brown-Peterson NJ, Wyanski DM, Saborido-Rey F, Macewicz BJ, Lowerre-Barbieri SK (2011) A standardized terminology for describing reproductive development in fishes. *Mar Coast Fish* 3(1):52–70. doi:10.1080/19425120.2011.555724
- Castro LR, Claramunt G, Krautz MC, Llanos-Rivera A, Moreno P (2009) Egg trait variation in anchoveta *Engraulis ringens*: a maternal response to changing environmental conditions in contrasting spawning habitats. *Mar Ecol Prog Ser* 381:237–248. doi:10.3354/meps07922
- Clarke TA (1989) Seasonal differences in spawning, egg size, and early development time of the Hawaiian anchovy or nehu, *Encrasicolina purpurea*. *Fish Bull* 87:593–600
- Coward K, Bromage NR (1998) Histological classification of oocyte growth and the dynamics of ovarian recrudescence in *Tilapia zillii*. *J Fish Biol* 53:285–302. doi:10.1111/j.1095-8649.1998.tb00981.x
- Emerson LS, Greer Walker M, Witthames PR (1990) A stereological method for estimating fish fecundity. *J Fish Biol* 36:721–730. doi:10.1111/j.1095-8649.1990.tb04326.x
- Erickson DL, Hightower JE, Grossman GD (1985) The relative gonadal index: an alternative index for quantification of reproductive condition. *Comp Biochem Physiol A* 81:117–120
- Funamoto T, Aoki I (2002) Reproductive ecology of Japanese anchovy off the Pacific coast of eastern Honshu, Japan. *J Fish Biol* 60:154–169. doi:10.1111/j.1095-8649.2002.tb02395.x
- Ganias K, Somarakis S, Machias A, Theodorou A (2003) Evaluation of spawning frequency in a Mediterranean sardine population. *Mar Biol* 142:1169–1179. doi:10.1007/s00227-003-1028-5
- Ganias K, Somarakis S, Machias A, Theodorou A (2004) Pattern of oocyte development and batch fecundity in the Mediterranean sardine. *Fish Res* 67:13–23. doi:10.1016/j.fishres.2003.08.008
- Howard C, Reed MG (1998) *Unbiased stereology: three dimensional measurements in microscopy*. BIOS Scientific Publishers, Oxford
- Hunter JR, Goldberg SR (1980) Spawning incidence and batch fecundity in northern anchovy, *Engraulis mordax*. *Fish Bull* 77:641–652
- Hunter JR, Leong R (1981) The spawning energetics of female northern anchovy, *Engraulis mordax*. *Fish Bull* 79:215–230
- Hunter JR, Macewicz BJ (1985) Measurement of spawning frequency in multiple spawning fishes. In: Lasker R (ed) *An egg production method for estimating spawning biomass of pelagic fish: application to the Northern Anchovy, Engraulis mordax*. NOAA technical report NMFS 36, pp 79–93
- Hunter JR, Lo NCH, Leong RJH (1985) Batch fecundity in multiple spawning fishes. In: Lasker R (ed) *An egg production method for estimating spawning biomass of pelagic fish: application to the Northern Anchovy, Engraulis mordax*. NOAA technical report NMFS 36, pp 67–77
- Hunter JR, Macewicz BJ, Lo NC, Kimbrell CA (1992) Fecundity, spawning, and maturity of female Dover sole *Microstomus pacificus*, with an evaluation of assumptions and precision. *Fish Bull* 90:101–128
- Imai C, Tanaka S (1994) Analysis of ovarian egg size frequency distribution of Japanese anchovy using computer graphics. *Fish Sci* 60:695–701

- Jons GD, Miranda LE (1997) Ovarian weight as an index of fecundity, maturity and spawning periodicity. *J Fish Biol* 50:150–156. doi:[10.1111/j.1095-8649.1997.tb01347.x](https://doi.org/10.1111/j.1095-8649.1997.tb01347.x)
- Kawaguchi K, Yamashita Y, Hayashi A (1990) Some aspects of spawning of the reared Japanese anchovy (*Engraulis japonicus* H.) in relation to the photoperiod, water temperature and starvation. *Bull Jpn Soc Fish Oceanogr* 54:364–372
- Korta M, Murua H, Kurita Y, Kjesbu OS (2010) How are the oocytes recruited in an indeterminate fish? Applications of stereological techniques along with advanced packing density theory on European hake (*Merluccius merluccius* L.). *Fish Res* 104:56–63. doi:[10.1016/j.fishres.2010.01.010](https://doi.org/10.1016/j.fishres.2010.01.010)
- Kurita Y, Kjesbu OS (2009) Fecundity estimation by oocyte packing density formulae in determinate and indeterminate spawners: Theoretical considerations and applications. *J Sea Res* 61:188–196. doi:[10.1016/j.seares.2008.10.010](https://doi.org/10.1016/j.seares.2008.10.010)
- Luo J, Musick J (1991) Reproductive biology of the Bay anchovy, *Anchoa mitchilli*, in Chesapeake Bay. *Trans Amer Fish Soc* 120:710–801
- Motos L (1996) Reproductive biology and fecundity of the Bay of Biscay anchovy population (*Engraulis encrasicolus* L.). *Sci Mar* 60(Suppl. 2):195–207
- Murua H, Saborido-Rey F (2003) Female reproductive strategies of marine fish species of the North Atlantic. *J Northw Atl Fish Sci* 33:23–31
- Palomera I, Pertierra JP (1993) Anchovy spawning biomass estimate by the daily egg production method in 1990 in the Western Mediterranean Sea. *Sci Mar* 57:243–251
- Somarakis S (2005) Marked inter-annual differences in reproductive parameters and daily egg production of anchovy in the northern Aegean Sea. *Belg J Zool* 135:247–252
- Somarakis S, Ganias K, Tserpes G, Koutsikopoulos C (2004a) Ovarian allometry and the use of the gonadosomatic index: a case study in the Mediterranean sardine, *Sardina pilchardus*. *Mar Biol* 146:181–189. doi:[10.1007/s00227-004-1419-2](https://doi.org/10.1007/s00227-004-1419-2)
- Somarakis S, Palomera I, Garcia A, Quintanilla L, Koutsikopoulos C, Uriarte A, Motos L (2004b) Daily egg production of anchovy in European waters. *ICES J Mar Sci* 61:944–958. doi:[10.1016/j.icesjms.2004.07.018](https://doi.org/10.1016/j.icesjms.2004.07.018)
- Somarakis S, Schismenou E, Siapatis A, Giannoulaki M, Kallianiotis A, Machias A (2011) High variability in the daily egg production method parameters of an eastern Mediterranean anchovy stock: influence of environmental factors, fish condition and population density. *Fish Res*. doi:[10.1016/j.fishres.2010.11.027](https://doi.org/10.1016/j.fishres.2010.11.027)
- Somarakis S, Tsianis DE, Machias A, Stergiou, KI (2006) An overview of biological data related to anchovy and sardine stocks in Greek waters. In: Palomares MLD, Stergiou KI, Pauly D (eds) *Fishes in databases and ecosystems*. Fisheries centre research reports 14, pp 56–64. Fisheries Centre, University of British Columbia
- Thorsen A, Kjesbu OS (2001) A rapid method for estimation of oocyte size and potential fecundity in Atlantic cod using a computer-aided particle analysis system. *J Sea Res* 46:295–308. doi:[10.1016/S1385-1101\(01\)00090-9](https://doi.org/10.1016/S1385-1101(01)00090-9)
- Uriarte A, Alday A, Santos M, Motos L (2011) A review of the spawning fraction estimation procedures for species with short spawning intervals: the case of the Bay of Biscay anchovy. *Fish Res*. doi:[10.1016/j.fishres.2011.03.002](https://doi.org/10.1016/j.fishres.2011.03.002)
- Witthames PR, Thorsen A, Murua H, Saborido-Rey F, Greenwood LN, Dominguez-Petit R, Korta M, Kjesbu OS (2009) Advances in methods for determining fecundity: application of the new methods to some marine fishes. *Fish Bull* 107:148–164